

Mechanical and microstructural investigations on cement-treated expansive organic subgrade soil

Nazerke Sagidullina^{1a}, Jong Kim^{1b}, Alfredo Satyanaga^{1c}, Taeseo Ku^{2d} and Sung-Woo Moon^{*1}

¹Department of Civil and Environmental Engineering, Nazarbayev University, Astana, 010000, Kazakhstan

²Department of Civil and Environmental Engineering, Konkuk University, Seoul, 05029, Korea

(Received March 5, 2024, Revised July 12, 2024, Accepted July 15, 2024)

Abstract. Organic soils pose significant challenges in geotechnical engineering due to their high compressibility and low stability, which can result in issues like differential settlement, rutting, and pavement deformation. This study explores effective methods for stabilizing organic soils. Rather than conventional ordinary Portland cement (OPC), the focus is on using environmentally friendly calcium sulfoaluminate (CSA) cement, known for its rapid setting, high early strength development, and environmental benefits. Mechanical behavior is analyzed through 1-D free swell, unconfined compressive strength (UCS), and bender element (BE) tests. Microstructural analyses, including Fourier transform infrared spectroscopy (FTIR) and scanning electron microscopy (SEM), characterize the soil mixed with CSA cement. Experimental results demonstrate improved soil properties with increasing cement dosage and curing periods. A notable strength increase is observed in soil samples with 15% cement content, with UCS doubling after 7 days. This trend aligns with shear wave velocity results from the BE test. SEM and FTIR spectroscopy reveal how CSA cement hydration forms hydrated calcium silicate gel and ettringite, enhancing soil properties. CSA cement is recommended for reinforcing organic subgrade soil due to its eco-friendly nature and rapid strength gain, contributing to improved durability.

Keywords: calcium sulfoaluminate cement; compressive strength; free swell; organic soil; shear wave velocity; soil stabilization; unconfined

1. Introduction

Organic soil is one of the problematic soils in geotechnical applications due to its high compressibility and low stability (Mitchell and Soga 2005). It consists of a mixture of soft clay and organic substances may also contain some visible pieces of partially decayed vegetation (Saride *et al.* 2013). The attributes of organic soils deviate from the conventional principles of soil behavior, presenting considerable challenges to civil engineering design. Typically, the presence of organic matter in soils correlates with heightened compressibility, notable secondary compression, and insufficient strength characteristics. For example, elevated compressibility and creep tendencies often elevate the risk of unacceptable settlement or foundation failure. Additionally, the deficient strength properties linked with lower maximum dry density

represent a significant issue in road construction (Huang *et al.* 2009). Therefore, improving organic soil properties is crucial in designing the subgrade layer since it affects pavement performance. For example, if the subgrade layer of organic soil is not adequately stabilized, it can lead to pavement serviceability problems such as differential settlement, rutting, and pavement deformation.

The classification of soil as organic soil in geotechnical engineering depends on the presence of the organic substances in the soil affecting the engineering behavior of soil. There are various available classification systems for the determination of organic soil. For example, the American Society for Testing and Materials (ASTM) standard classification states that when the amount of organic matter is below 75% of the dry mass, the soil is classified as organic soil (ASTM/D2487 2000). Moreover, organic soil can be classified by utilizing the liquid limit (LL) values as per the Unified Soil Classification System, wherein the LL of oven-dried soil specimens should not surpass 75% of the LL measured from air-dried soil samples (García-Gaines and Frankenstein 2015). Furthermore, it was found that even small amounts of organic matter can adversely affect soil's chemical and engineering properties due to its colloidal behavior (Edil and Wang 2000).

A common technique for improving subgrade soil properties is using calcium-based additives to stabilize the problematic soils chemically (Regasa *et al.* 2023). It can enhance the features of strength and volume change of the soil. The concept of employing calcium-based additives to stabilize soils aims to enhance their engineering properties.

*Corresponding author, Associate Professor

E-mail: sung.moon@nu.edu.kz

^aGraduate Student

E-mail: nazerke.sagidullina@nu.edu.kz

^bProfessor

E-mail: jong.kim@nu.edu.kz

^cAssociate Professor

E-mail: alfredo.satyanaga@nu.edu.kz

^dAssociate Professor

E-mail: tsku@konkuk.ac.kr

The primary reaction involved is cement hydration. When water is present, soil particles react with the cement, leading to the formation of cementitious compounds like calcium silicate hydrate (C-S-H) and calcium aluminate hydrate (C-A-H) over time. This chemical reaction contributes to the strength development and cohesion of the stabilized soil (Firoozi *et al.* 2017, Ahmadullah and Chrysochoou 2024).

Ordinary Portland cement is extensively utilized in geotechnical engineering due to its satisfactory mechanical properties, material availability, and cost-effectiveness. Numerous researchers have thoroughly documented the benefits of using cement for soil stabilization (Prusinski and Bhattacharja 1999, Horpibulsuk *et al.* 2006, Niazi and Jalili 2009, Ma and Zhang 2014, Ifedimiro and Ekeocha 2022). For example, treating the soil with OPC enhances its bearing capacity and reduces its permeability and compressibility (Kamruzzaman *et al.* 2009, Horpibulsuk *et al.* 2010, Vinoth *et al.* 2018). However, the use of OPC causes serious environmental problems due to the high carbon dioxide content produced during cement production, depletion of natural resources due to the extraction of raw materials such as limestone and clay, and dust generation during the production process. Approximately 4.5% of carbon emissions can be directly referred to OPC (GCB 2023), with 800 kg of CO₂ produced for every ton of cement (Damtoft *et al.* 2008, Winnefeld and Lothenbach 2010). In addition to environmental concerns, OPC often exhibits high plastic shrinkage and reduced mechanical strength due to water loss and incomplete hydration in the early stages. Consequently, this represents a significant disadvantage for geotechnical applications, especially in hot regions where large-scale wet curing is not practical (Bushlaibi and Alshamsi 2002).

Due to the increasing annual consumption of cement, there is a need to change commonly used OPC-based approaches with more eco-friendly methods. Many researchers have explored various soil stabilizers in combination with traditional binders to reduce the emission of carbon gases while improving the properties of problematic weak soils. These soil stabilizers, such as furnace slag, fibers, fly ash, kiln dust, silica fume, rice husk and geopolymers, have shown a considerable improvement in strength (Phanikumar 2009, Ghazavi and Roustaie 2010, Arasan and Nasirpur 2015, Zhang *et al.* 2016, Güllü and Fedakar 2017, Jexembayeva *et al.* 2020, Mekonnen *et al.* 2022, Ale 2023, Ghadr *et al.* 2023, Gidebo *et al.* 2023, Mustafayeva *et al.* 2023, Olagunju *et al.* 2023, Zivari *et al.* 2023).

This experimental research focused on calcium sulfoaluminate (CSA) cement, a sustainable product that can replace OPC, as it has a low carbon footprint, quick strength gain, and small shrinkage. It's important to note that CSA cement can indeed replace ordinary Portland Cement (OPC) entirely in specific applications. In contrast, other alternative materials may only partially replace OPC to achieve the required engineering properties (Hanein *et al.* 2018). This distinction underscores the versatility and potential environmental benefits of CSA cement, as it offers a viable alternative that can reduce or eliminate the reliance on OPC, thereby further reducing the overall environmental

impact associated with cement production. Moreover, it requires less heat during production, and its main constituents generate 62.7% fewer carbon gases than OPC. Numerous studies have demonstrated the effectiveness of CSA cement for soil stabilization purposes. For instance, Vinoth *et al.* (2018) explored the suitability of CSA cement for rapid and environmentally friendly treatment methods. Their research revealed that sand treated with CSA cement exhibited significantly higher compressive strength, ranging from 2 to 9 times greater compared to sand treated with OPC, with variations based on calcium sulfate levels and cement content. Additionally, they conducted mechanical and microstructural analyses on sand treated with CSA cement, comparing curing conditions in wet and dry settings (Subramanian *et al.* 2018). Results indicated that both OPC-treated and CSA-treated sand samples cured underwater exhibited lower strength compared to dry-cured samples. However, the decrease in strength due to wet curing was less pronounced for CSA-treated sand compared to OPC-treated sand. Furthermore, CSA cement demonstrated durability against aggressive environments (Moon *et al.* 2020, Bisserik *et al.* 2021, Jumassultan *et al.* 2021, Ocheme *et al.* 2023). Additionally, Pooni *et al.* (2020) and Sagidullina *et al.* (2022) conducted research to examine the efficacy of CSA cement in addressing challenging soil conditions, showing favorable outcomes.

Although several studies have investigated the application of CSA cement for soil improvement purposes, its effectiveness in stabilizing organic soils has not yet been studied. Organic soils tend to exhibit poor engineering properties such as low bearing capacity and high compressibility. The rapid setting and early strength development of CSA cement will allow for faster stabilization of organic soils, minimizing construction time and increasing structural stability. This research aims to examine the application of CSA cement on organic soil to examine its strength improvement behavior under various curing times and cement contents. The mechanical behavior of CSA-treated soil is investigated through unconfined compressive strength (UCS), bender element tests, and the one-dimensional (1-D) free swell test. The CSA-treated soil is characterized using microstructural techniques, including Fourier transform infrared spectroscopy (FTIR) and scanning electron microscopy (SEM). The study offers a comprehensive understanding of strength development for the organic soil stabilized with CSA cement. This understanding can support the modification and stabilization of organic soils in the construction of environmentally friendly road infrastructure, thereby reducing the environmental impact associated.

2. Materials

2.1 Natural soil

The natural soil used in this research was taken from a land excavation site in Astana, Kazakhstan. Prior to stabilization investigations, a number of laboratory tests were conducted on the soil to first categorize it and then

Table 1 Physical properties of natural soil

Property	Value	Standard
D10 (mm)	0.08	
D30 (mm)	0.18	
D60 (mm)	0.45	ASTM D1921
Coefficient of curvature	0.90	
Coefficient of uniformity	5.63	
USCS classification	SP-SM	
Liquid limit (%)	84	ASTM D4318
Plastic limit (%)	74	ASTM D4318
Plasticity Index (%)	10	ASTM D4318
Optimum moisture content (%)	36	ASTM D698
Maximum dry density (kN/m ³)	1.116	ASTM D698
Organic Content (%)	19	ASTM D7348-21
Expansion Index	71 (medium)	ASTM D4829-03

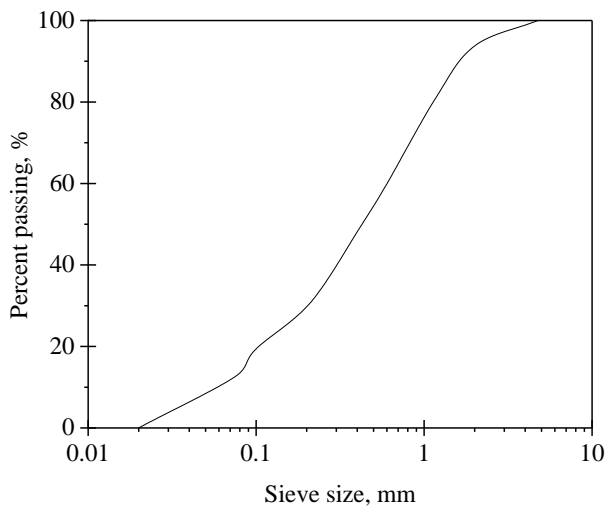


Fig. 1 Grain size distribution curve

figure out the best stabilizer doses for each sample. Table 1 shows the list of basic geotechnical properties of the natural soil. The particle size distribution curve of the soil used in the research is illustrated in Fig. 1. Soil type is classified according to ASTM standards and the USCS classification system. Additionally, employing Atterberg limit and sieve analysis techniques within these classification systems enhances our comprehension of soil behavior. Based on the Unified Soil Classification system (USCS), the soil is classified as poorly-graded sand with silt (SP-SM).

The X-ray diffraction (XRD) test was conducted to analyze the materials' mineralogy and crystalline structure. The testing result shows that the soil mainly comprises quartz, illite, and kaolinite in Fig. 2(a). The oxide chemistry of natural soil obtained from an X-ray fluorescence (XRF) spectrometer is illustrated in Table 2. XRF provides information on the elemental composition of a material, which can be used to identify potential phases that may be

present in the sample. XRD can then be used to confirm the presence of these phases and determine their crystal structure. The presence of organic matter in soil was identified through visual inspection and olfactory examination. The soil exhibited a darker color, indicative of organic content, and emitted an earthy odor, particularly when moist. To determine the organic content (OC) of the soil, the loss on ignition (LOI) test was performed (ASTM/D7348 2013). Soil with OC of 2% to 6% is categorized as having low organic content, whereas soil containing 6% to 20% OC is considered to have medium organic content (Myślińska 2003). The OC of the natural soil was 19%, classified as soil with a medium organic content.

Moreover, to determine the expansiveness of organic soil, The expansion index (EI) test was conducted based on ASTM Standards (ASTM/D4829 2003). The Expansion Index (EI) test evaluates the potential volume change or expansion of a soil sample subjected to moisture variation. The soil material is first sieved using a No. 4 sieve and then adjusted to achieve optimum moisture content, typically between 80% and 85% saturation. After a settling period of 6 to 30 hours, the moisture-treated soil is compacted in two layers into a mould with a diameter of 10.19 cm and a height of 2.54 cm. If necessary, the moisture content is further adjusted to a saturation level of 50%. A load of 6.9 kPa is then applied, and the sample is wetted and monitored for 24 hours to measure the resulting volumetric swelling. The resulting volume changes are measured and used to calculate the expansion index, which quantifies the soil's susceptibility to swell or shrink under varying moisture conditions. The expansion index of organic soil was 71.1, indicating a moderately expansiveness according to classification standards (ASTM/D4829 2003).

2.2 Calcium sulfoaluminate (CSA) cement

CSA cement utilized as a primary admixture to stabilize the organic soil mainly comprises ye'elimite, anhydrite, and belite, as shown in Fig. 2(b). CSA cement offers several advantages over OPC in soil stabilization applications: (1) much faster setting time; (2) early strength development; (3) fewer CO₂ emissions than OPC, making it a more environmentally friendly option (Subramanian et al. 2018). Treatment of problem soils with CSA cement primarily relies on the chemical mechanism of hydration reactions. The hydration process of CSA cement is complex and depends on the gypsum or anhydrite content of the binder. Depending on the concentration of gypsum, the reaction results in the formation of either ettringite ($C_3A \cdot 3CS \cdot 32H$) or monosulfate ($C_3A \cdot CS \cdot 12H$). Ettringite forms when there is a high concentration of gypsum during early hydration, while monosulfate forms when the gypsum concentration is low or depleted (Vinoth et al. 2018). Additionally, the sustainable high initial strength was achieved by replacing 30% of CSA cement with gypsum, as the reaction between ye'elimite and gypsum at a very early stage results in the growth of needle-like ettringite crystals, which results in a rapid increase in strength (Ku et al. 2020).

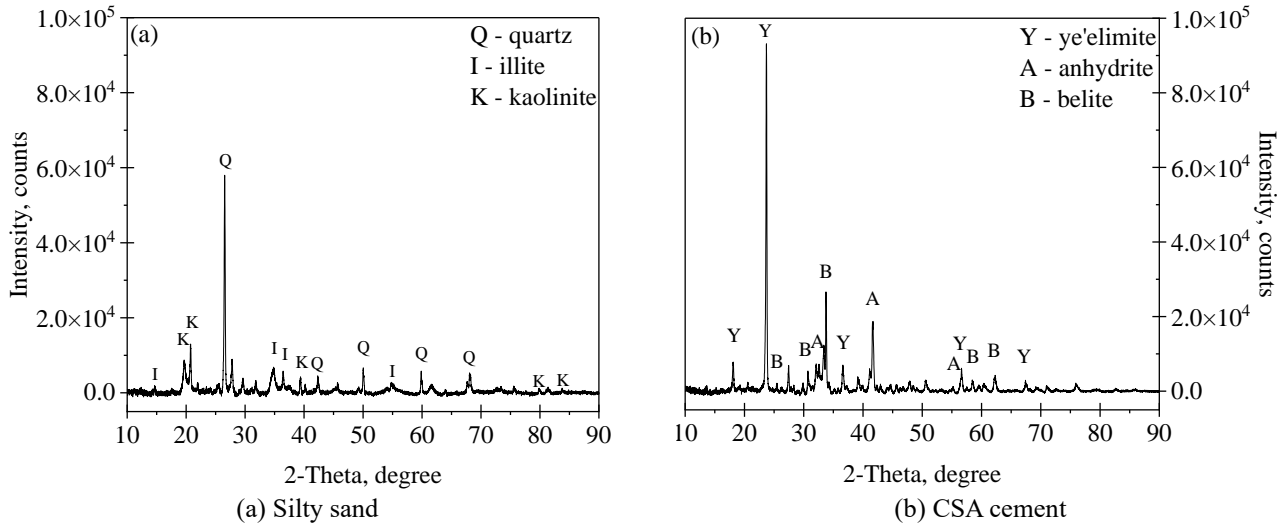


Fig. 2 X-Ray Diffraction (XRD) analysis

Table 2 Chemical composition of CSA cement and natural soil

Chemical composition	CSA cement	Soil
MgO	1.266	1.053
Al ₂ O ₃	14.319	33.829
SiO ₂	49.032	7.956
SO ₃	5.679	8.461
K ₂ O	2.925	0.617
CaO	4.017	41.042
MnO	0.079	7.918
Fe ₂ O ₃	6.228	1.709

The oxide chemistry of the cement is illustrated in Table 2. Using the data about elemental composition of the cement, the potential phases were determined. The XRD result of CSA cement shows that the cement mainly composes of ye'elimite, anhydrite and belite, quartz in Fig. 2(b).

3. Mix design and sample preparation

The mixture of CSA cement and soil was made at the optimum moisture content (OMC). This study investigated various cement proportions, specifically 0%, 5%, 10%, and 20% cement content. The OMC and corresponding maximum dry densities (MDD), obtained from the standard Proctor test (ASTM/D698 2021), are illustrated in Fig. 3. The results of the OMC were 36%, 41%, 44%, and 45.5%, and the results of the MDD were 1.115, 1.105, 1.101, and 1.062, for the samples treated with 0%, 10%, 15%, and 20% CC, respectively. It can be noticed that with the raise of cement content (CC) from 0% to 20%, the OMC increases, and MDD decreases.

The experimental study commenced with the determination of cement content by accurately measuring the cement within the dry soil mass. Next, the gypsum

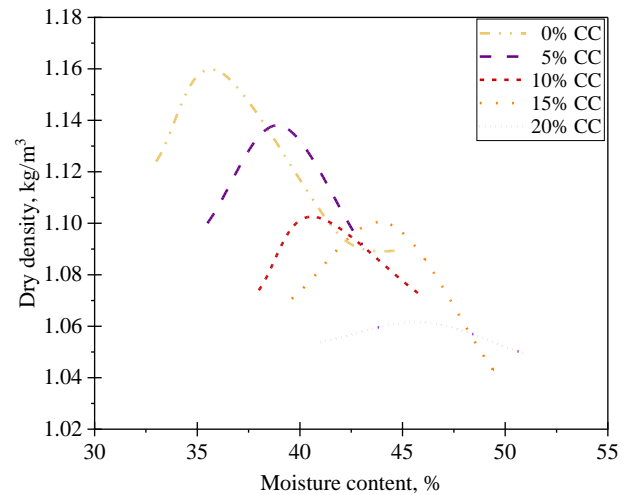


Fig. 3 Moisture content and dry density relationship, CC - cement content

content was calculated by evaluating the quantity of gypsum within the entire binder's mass. Water content was then determined by dividing the mass of water by the total mass of solids, which included soil and binder. Following these content calculations, samples were prepared for subsequent analysis. The mixing process consisted of two steps: first, blending the dry ingredients together, and then adding water to the mixture.

Following the preparation of soil-cement mixture, soil samples treated with cement were formed using a mould with dimensions of 50 mm × 100 mm, in diameter and height. The soil samples were meticulously prepared employing the undercompaction technique to ensure uniform density across all layers, with each layer being compacted 25 times using a hand rammer (Ladd 1978). Moreover, during compaction, the top and middle layers were scarified to ensure adequate contact between soil layers. To enhance the reliability of the experimental results, three samples were prepared for each combination. Subsequently, the samples were left in the mold for 24

Table 3 Testing program

Test sample	Test	Standard	Curing period
All samples	1-D Free Swell	ASTM/D4546 (2014)	3, 7, 14 and 28 days
	Bender element	-	
	UCS test	ASTM/2166 (2003)	
	FTIR spectroscopy	-	
Samples with 0, 10, 15, and 20% CC	SEM test	-	3 days
Samples with 20%			3, 7, 14 and 28 days

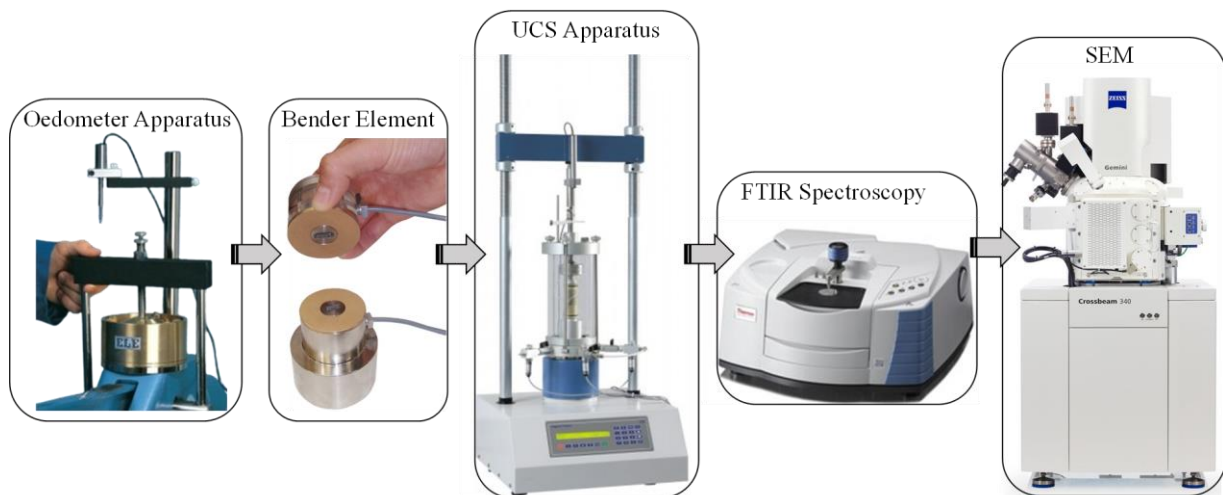


Fig. 4 Experimental set up

hours before being extruded and then wrapped in plastic film. The specimens were left to cure at room temperature for 3, 7, 14, and 28 days using the dry curing method, which may lead to changes in the degree of saturation. However, the effect of matrix suction on the test specimens is not considered significant within this test procedure (Consoli *et al.* 2007, Wei *et al.* 2022).

4. Testing procedure

To obtain a comprehensive understanding of the hydro-chemo-mechanical characteristics of CSA-treated soil, a total of five primary experiments were conducted. These experiments, namely one-dimensional (1-D) free swell, bender element (BE), unconfined compressive strength (UCS), Fourier transform infrared (FTIR) spectroscopy, and scanning electron microscope (SEM) tests, aimed to investigate various properties such as swelling (volume change), stiffness, strength, chemical composition, and microstructures. The testing program and conditions are outlined in Table 3, while the experimental setup is illustrated in Fig. 4.

4.1 1-D free swell test

After completion of the curing periods, a one-dimensional free swell test is performed using an oedometer

in accordance with ASTM standard (ASTM/D4546 2014). This laboratory test aims to evaluate soil swelling potential, which is essential for understanding soil behavior under varying moisture conditions. The test involves measuring the volumetric expansion of a soil sample as it absorbs water under free swelling conditions. Initially, a soil sample is carefully placed into a cylindrical mold with a diameter of 50 cm and a height of 20 cm, ensuring uniform compaction. Subsequently, the sample is fully saturated with water to simulate field conditions. A porous stone is then positioned atop the soil sample to facilitate unimpeded swelling. Throughout a defined period, the height of the soil sample is meticulously monitored. This observation allows for the determination of the amount of free swelling, computed as the ratio of the increase in height to the initial height of the soil sample. Such quantitative analysis furnishes valuable insights into the expansion characteristics of soils during hydration. The free swell test is conducted until the soil sample attains a state of stability, thereby yielding accurate and reliable results.

4.2 Bender element (BE) test

Fig. 4 shows that the shear wave velocity of soil samples was measured using bender elements (BEs) after the curing days were complete. It comprises two parallel metal plates separated by a thin piezoelectric material layer (GSD Bender Element system) (ASTM/D8295 2019).

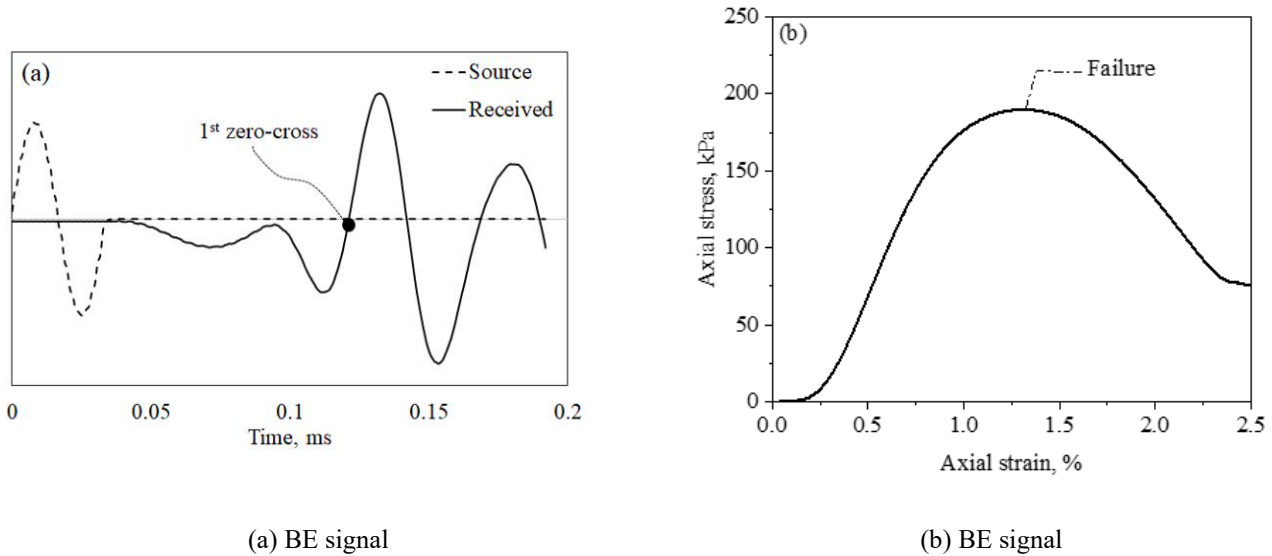


Fig. 5 Representative test results for the BE and UCS tests (cement content = 10%, curing day = 7 days)

When an electrical signal is applied to the piezoelectric material, it causes the bender to vibrate, generating a shear wave propagation through the soil surrounding the element. Two grooves are made on each side of the sample to install the benders. The BEs are then placed into the grooves and firmly secured with the filler material. This ensures that the BEs make good contact with the sample. During the test, both transmitted and received signals are captured and recorded using computer software. The recorded data provides valuable insights into the soil's mechanical properties, aiding in the characterization of its stiffness and shear strength (Khan *et al.* 2020). The shear wave velocity for each sample was determined using the first zero-cross at a frequency of 30 kHz, as shown in Fig. 5(a). In interpreting the first arrival of the shear wave, the adopted approach was demonstrated for cement-treated soil with similar stiffness (Wei *et al.* 2022)

4.3 Unconfined compressive strength (UCS) test

After measuring the shear wave velocity values, the soil samples were tested in a universal compression apparatus with a standard deformation rate of 1 mm per minute (Digital Tritest 50 Load Frame). This evaluation of compressive strength, known as the unconfined compressive strength (UCS) test, adheres to the guidelines outlined in ASTM/D2166 (2006). During the UCS test, the compressive strength of the specimen was determined by analyzing the peak stress reached during testing. To increase the reliability and representativeness of the results, the average of the results for three separate samples was calculated and used for data analysis.

The stress-strain relationship obtained from the UCS test provides valuable information about the mechanical behavior of the soil under compression. Fig. 5(b) illustrates a representative stress-strain curve obtained from a UCS test, demonstrating the relationship between the applied stress and the corresponding strain.

4.4 Fourier Transform Infrared (FTIR) spectroscopy

Fourier transform infrared spectroscopy (FTIR) serves as a key tool in the analysis of soil samples to define the chemical composition of both untreated and treated soil. Using FTIR, researchers can distinguish and evaluate different types of chemical bonds present in treated soil, providing insight into structural modifications and interactions between soil components and cementitious materials (Chub-upakarn *et al.* 2023). After completion of the UCS test, small portions of the test samples are subjected to FTIR analysis. To ensure accurate results, soil samples are first oven dried to remove any moisture content that may interfere with spectroscopic measurements. FTIR spectra are obtained using a Nicolet iS10 FTIR spectrometer, which can accurately measure and characterize chemical bonds in soil samples. The resulting spectra facilitate the identification of specific functional groups and chemicals present in the soil, which helps to better understand the effects of treatment technique on soil composition and structure.

4.5 Scanning electron microscope (SEM)

The scanning electron microscope (SEM) is used to observe changes in the microstructure of the untreated soil and the soil treated with CSA cement at different curing periods. SEM provides valuable visual information about soil microstructure at higher magnification, facilitating the assessment of changes in particle morphology, distribution, and formation of cementitious phases. Before SEM images are captured, soil samples undergo a coating process with a thin layer of gold alloy. This coating improves image quality by reducing charge effects and improving conductivity. SEM ZEISS Crossbeam 540 apparatus is applied for the microstructural analysis of soil.

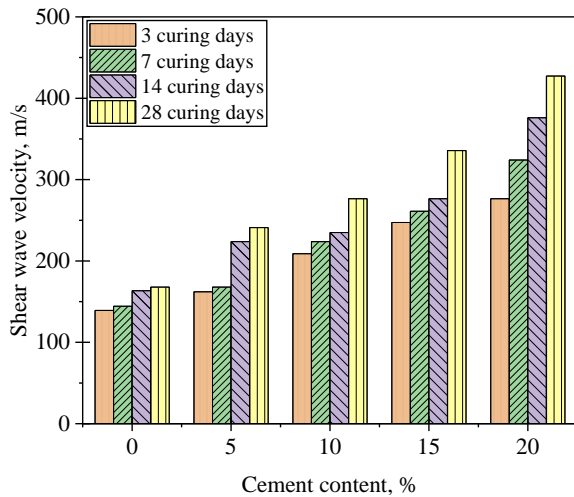


Fig. 6 Bender Element test results

5. Results

5.1 Mechanical behavior

5.1.1 Bender Element (BE)

Fig. 6 shows the variation of shear wave velocity with respect to cement content. Generally, the shear wave velocity (V_s) demonstrates an upward trend with increasing cement content, ranging from 0% to 20%, and with increasing curing time from 3 to 28 days. For instance, at various cement dosages, the V_s shows noticeable increases over the curing period. Specifically, at 5% cement content, V_s rose from 162.1 m/s to 241 m/s; at 10%, it increased from 187 m/s to 277 m/s. At 15% and 20% cement content, the velocity similarly increased from 267 m/s to 336 m/s and from 277 m/s to 427 m/s, respectively, from 3 to 28 day curing period. Significantly, the V_s exhibited rapid enhancement, notably at 15% cement content, where it doubled after 7 curing days compared to the untreated sample. This observation underscores the soil's quick-strength gain property, indicative of the effectiveness of the cement treatment in enhancing soil stability. Thus, an increase in cement content correlates with an increase in shear wave velocity, thereby increasing the stiffness and strength of the soil. This relationship highlights the usefulness of cement stabilization in improving soil mechanical properties, which has implications for a variety of geotechnical applications.

5.1.2 Unconfined compressive strength (UCS)

This study investigated the relationship between the unconfined compressive strength (UCS) of soil and cement content at different curing periods. Fig. 7 illustrates that the UCS value increases with increased cement dosage and curing period. For example, soil samples with 5% cement content exhibited a 1.2-1.3 times strength increase compared to untreated soil, while samples with a cement content of 20% showed 3-5 times increase in strength, depending on the curing period. However, the difference in unconfined compressive strength (UCS) values was negligible between the 5% and 10% cement dosage

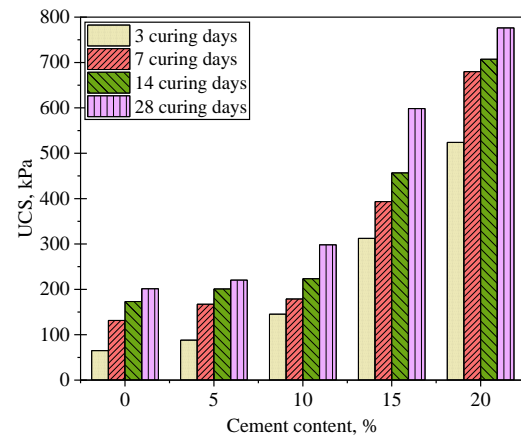


Fig. 7 Unconfined compressive strength (UCS) test results

specimens. In contrast, a significant improvement in strength was evident in the 15% cement treated samples, a trend also observed in the BE test results. The growth in strength can be referred to the chemical reactions occurring during the curing process of cement-treated soil.

The hydration of CSA cement leads to the formation of calcium sulfoaluminate hydrates. Nonetheless, consuming hydrated cement by organic matter can reduce the amount of hydration products. Organic matter in soil can also consume the water required for cement hydration, leading to a slower or even halted hydration process and reduced strength gain (Tremblay *et al.* 2002, Chen and Wang 2006). Additionally, organic matter can bind with cement particles, reducing the amount of cement available for the hydration process and ultimately resulting in reduced strength gain. This behavior of treated soil can be explained by the chemical reaction between cement and water resulting from the hydration of CSA cement and forms calcium silicate hydrate (C-S-H) gel and ettringite, a mineral formed during the early stages of cement hydration. This process allows it to bond with the soil particles resulting in a more stable and durable soil structure.

Fig. 8 presents the typical failure modes of broken samples after the UCS test. The failure plane of cement-treated soil shows brittle failure, where a cone-shaped pattern was observed. Overall, typical seven-day UCS for cement stabilized subgrade soil range from 0.68 to 2.07 MPa. So, the UCS value for the organic soil treated with 20% CSA cement after 7 curing days was 0.692 MPa, which meets the UCS requirements, where the typical 7-day UCS shown as 689 kPa (Gross and Adaska 2020).

5.1.3 Correlation between UCS and V_s

The conventional method for ensuring the quality of cement-stabilized soils involves conducting mechanical strength tests, which are destructive, expensive, and inconvenient when continuous monitoring is required. On the other hand, V_s measurement can be carried out quickly and non-destructively on-site, making it a useful indicator of strength development in cement-treated soils. Therefore, establishing a correlation between UCS and V_s is beneficial for quality control and monitoring purposes.

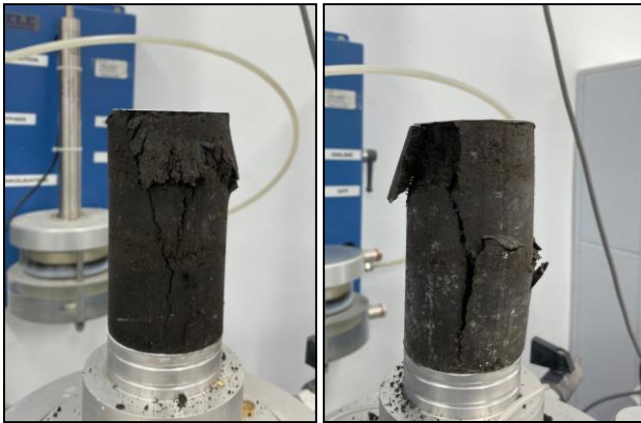


Fig. 8 Failure modes of soil samples after UCS test

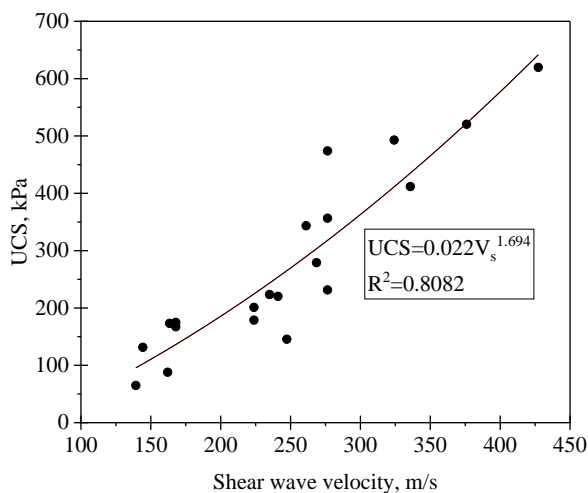


Fig. 9 Relationship between UCS and shear wave velocity

The V_s is commonly used as a standard quality control measure, with prior studies suggesting a correlation between V_s and UCS for cemented sands. Utilizing data from this study, a correlation model between V_s and UCS was developed, as shown in Fig. 9.

The findings reveal a consistent trend wherein UCS rises with escalating V_s (Moon *et al.* 2020, Sagidullina *et al.* 2022, Wei *et al.* 2022). Based on the available data in this study, we propose a useful correlation model between V_s and UCS, as shown in Fig. 9, and it was found that UCS generally increases as V_s increases. Fig. 9 presents the power relationship was established, and the empirical equation was developed to predict UCS from V_s , where the R^2 value was equal to 0.81. The coefficient of determination (R^2) value of 0.81 indicates a strong correlation between UCS and V_s , indicating the robustness of the proposed correlation model. This correlation model offers a practical tool for predicting UCS based on V_s measurements, facilitating effective quality control and monitoring of cement-stabilized soils. Given the established strong relationship between UCS and V_s if the UCS values meet the target criteria, we can infer that the shear wave velocity also meets the required standards.

5.2 Volume change behavior

5.2.1 Free swell

The free swell test is an important laboratory test used to evaluate the swelling potential of the soil and determine subgrade stabilization techniques. In practical applications, the free swell test can assess the potential for subgrade soils to cause heaving or distortion of the road surface (Puppala *et al.* 2005). The results showing free swelling percentage (FSP) for soil samples at different curing periods are presented in Fig. 10. The results of the free swell percentage for the soil samples at different curing periods are illustrated in Fig. 10. For the 3-days cured samples of untreated sand, the Free swell percentage (FSP) was 7.8%, whereas with the increase of cement dosage to 5%, 10%, 15%, and 20% the FSP decreased for 6.6%, 5.5%, 4.6%, and 1.6%, respectively. A consistent trend was observed for soil samples cured for 7, 14, and 28 days. Here, as the cement content increases from 0% to 20%, the FSP decreases from 3.8% to 0.8% for samples cured for 7 days, from 3.4% to 0.5% for samples cured for 14 days, and from 2.4% to 0.2% for samples cured within 28 days. Consequently, the percentage of free swelling becomes negligible with increasing cement dosage. According to the Sridharan and K.Prakash (2000), the soil with an FSP of less than 1% can be considered non-swelling. As shown in Fig. 10, the soil with 20% cement content meets this criterion. These results highlight the significant impact of curing time on swelling control. However, the percentage of cement used appears to be a more influential factor, especially at higher cement proportions. The results obtained from the free swell test follow a consistent trend observed in the UCS and BE tests, demonstrating that the effectiveness of the treatment increases with both the duration of curing days and the dosage of cement.

Based on the tests performed to characterize the mechanical properties of stabilized soil, it can be concluded that the CSA-treated organic soil has shown good performance in strength, shear wave velocity and swelling percentage. Moreover, it is essential to investigate the long-term effect and curing in wet conditions for organic soil treated with CSA cement. These aspects are of great importance for future research as they can significantly impact the strength and durability of the soil as time progresses. Furthermore, variables such as the conditions and duration of the curing process can substantially influence the characteristics of the soil, thereby affecting its effectiveness in different applications. Hence, conducting additional studies on the long-term effects and wet curing of CSA cement-treated organic soil can offer valuable knowledge for enhancing its performance and durability.

5.3 Microstructural behavior

5.3.1 FTIR

Fig. 11 presents the results of FTIR spectroscopy conducted on the soil samples for 3, 7, 14, and 28 days with different cement content.

FTIR is a useful analytical technique that can provide valuable information about the types of chemical bonds

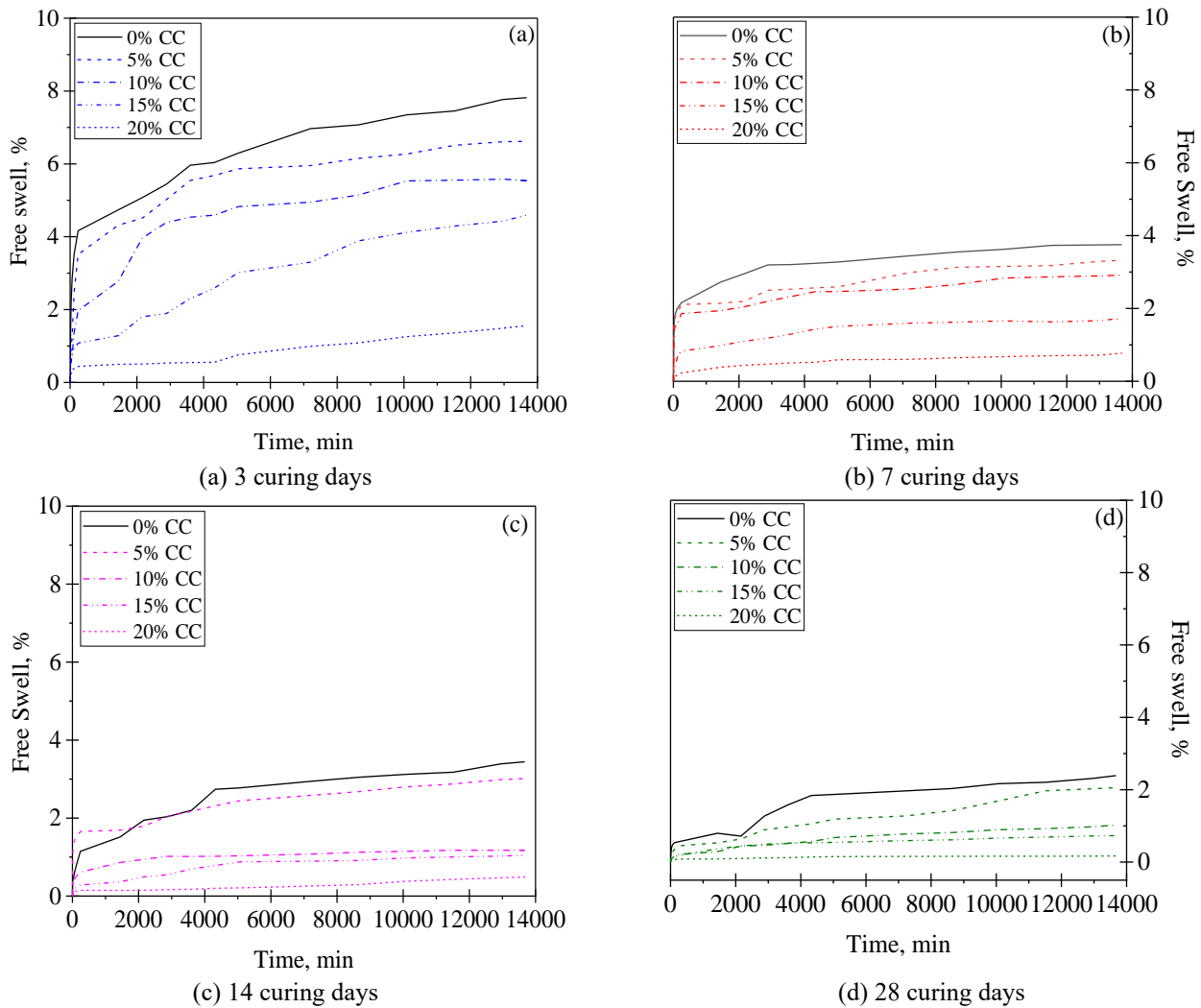


Fig. 10 1-D swell test results for natural soil and CSA cement stabilized samples [CC – cement content

present in treated soil, facilitating a comprehensive understanding of its structure and properties. The untreated soil in Fig. 11, shown as the control spectrum, has an absorption band at 3630 cm^{-1} and 3720 cm^{-1} , indicating the presence of kaolinite and weak bands at 710 cm^{-1} and 755 cm^{-1} , showing the presence of quartz minerals.

Furthermore, the absorption band at 910 cm^{-1} distinguishes the presence of illite mineral. Several changes occurred in the region caused by O-H groups (ranging from $4000\text{--}3000\text{ cm}^{-1}$) following curing soils cemented with CSA. It can be observed that the intensity of peaks at 3630 cm^{-1} and 3720 cm^{-1} was reduced. That was caused by the stretching vibrations of O-H groups that are present in ettringite, formed after the reaction between cement and water. The increase of ettringite shows the strength development of a treated soil.

The absorption band at 1680 cm^{-1} shows the presence of hydrated products. The presence of ettringite and an increase in its amount can be observed with the broadening of the adsorption area because of O-H groups. The intensity increase at 1510 cm^{-1} can be seen due to the carbonation of calcium present in CSA cement. The absorption band at

1680 cm^{-1} signifies the presence of hydrated products, crucial for the overall hydration process, facilitating binding and densification of soil particles, thus contributing to strength development in the soil-cement system. Moreover, the intensity increases at 1510 cm^{-1} , indicative of calcium carbonation in CSA cement, underscores the importance of this phenomenon in long-term durability and strength development, influencing soil stabilization mechanisms and performance

5.3.2 SEM

Fig. 12 shows the microstructure of the natural soil and CSA cement treated soil at different cement content after three curing days. The SEM pictures of untreated soil samples show the presence of voids and agglomerated soil particles, whereas the formation of needle-shaped structures can be observed from the CSA-treated soil samples.

This formation of ettringite, facilitated by increased cement dosage, contributes to higher density and lower porosity in the treated soil, consequently leading to expedited setting time and bolstered early strength (Subramanian *et al.* 2018).

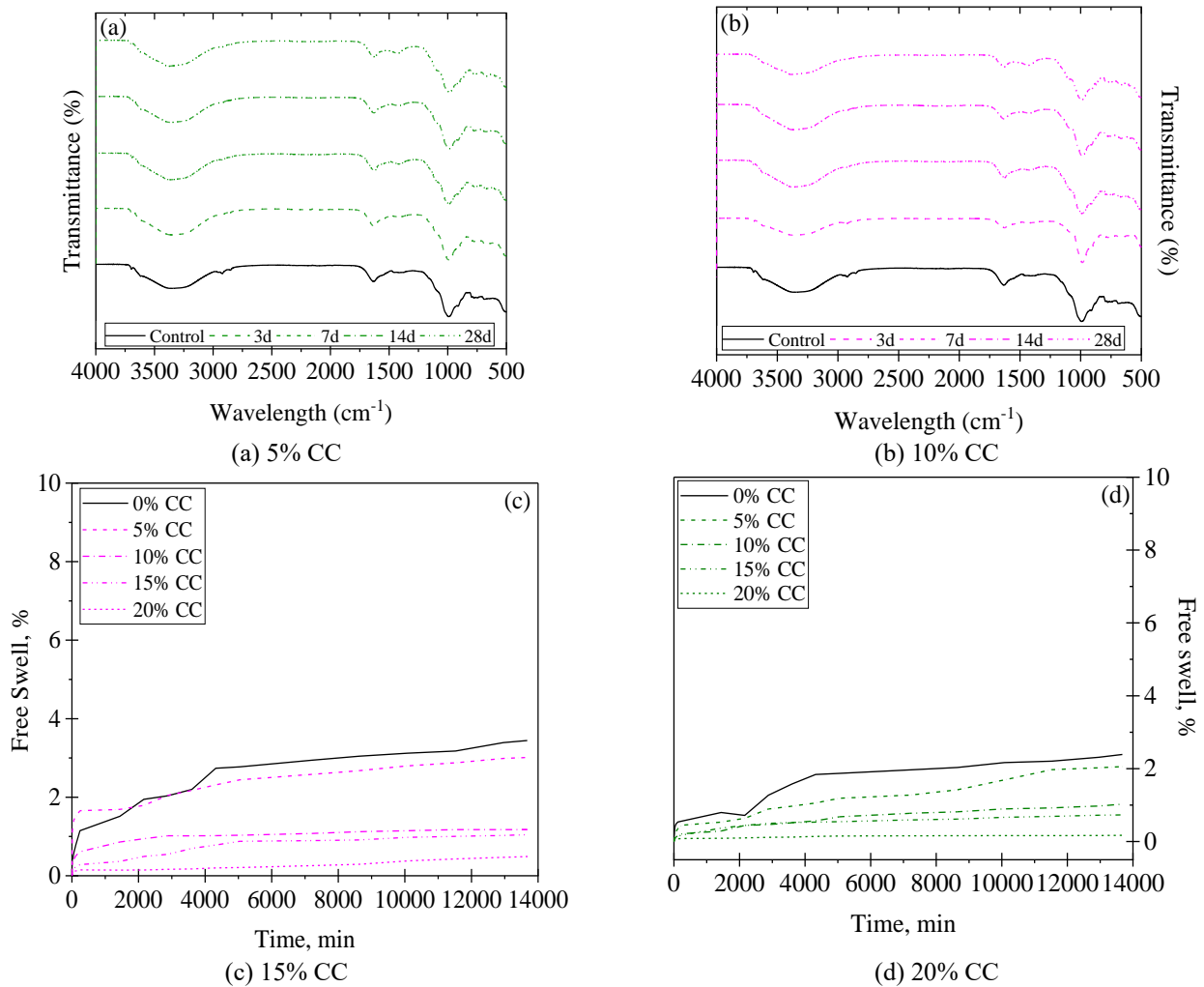


Fig. 11 FTIR spectrum of CSA-treated soil at different cement content [CC – cement content]

This phenomenon underscores the efficiency of CSA cement in enhancing soil properties. Moreover, Fig. 13 shows the SEM images of soil treated with 20% cement dosage at different curing periods. At higher cement dosages, there was a greater formation of well-developed ettringite, which is consistent with the results of FTIR spectroscopy, where ettringite formation is observed at 1680 cm^{-1} absorption band. The increased presence of ettringite at higher cement dosages highlights the effectiveness of CSA cement in helping to stabilize soils by forming strong interconnected crystals, which helps improve soil strength and durability.

Stronger bonding will be formed when the soil particles are completely interconnected with a high density of ettringites, as illustrated in Fig. 14. The organic soil has a substantial amount of water surrounding the soil particles, which reduces the density and strength of the soil. When CSA cement is added to organic soil, the stabilization process begins quickly. This leads to a rapid decrease in the thickness of the water layer and a subsequent decrease in the distance between soil particles (Horpibulsuk et al. 2010). As cementitious hydration occurs, ettringite needles fill the spaces, increasing the density and reducing porosity. This causes a quick setup time and early strength.

6. Conclusions

The research is conducted to evaluate the performance of calcium sulfoaluminate cement for improving organic soil properties by assessing the mechanical properties of treated soil. To assess the mechanical properties of stabilized soil, 1-D Free swell, UCS, and BE tests were performed, and the microstructural analysis was also carried out. The following main conclusion was made from this experimental research:

- The addition of CSA cement increased the V_s of treated organic soil. The V_s of stabilized soil increased by 16% for the soil with 5% cement dosage even after three curing days, which demonstrates the quick strength gain property of CSA cement.
- The UCS test results follow the trend as BE test, where soil strength raised with the increase of cement dosage and curing days. A practical correlation model was proposed for tracking strength development through non-destructive monitoring, where the coefficient of determination (R^2) value was 0.81 indicating a strong correlation between UCS and V_s .

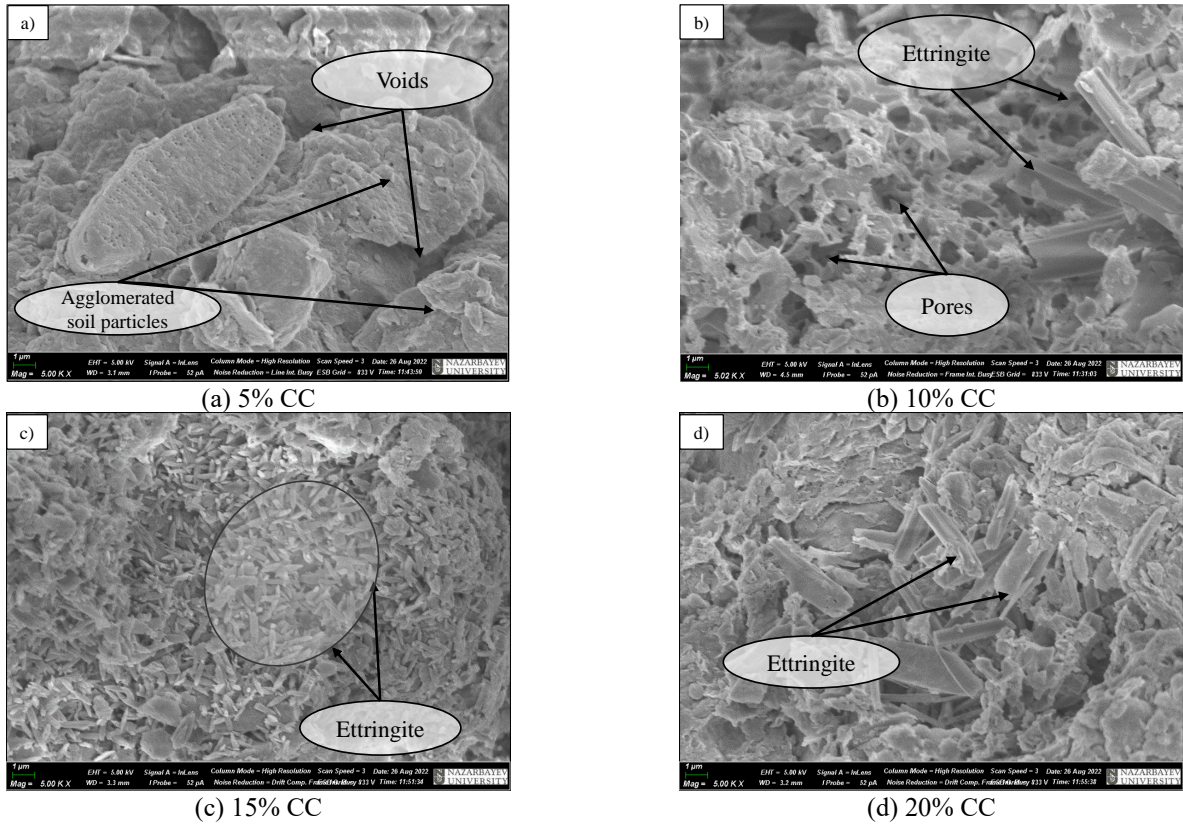


Fig. 12 SEM pictures of 3 day cured soil samples at different cement content

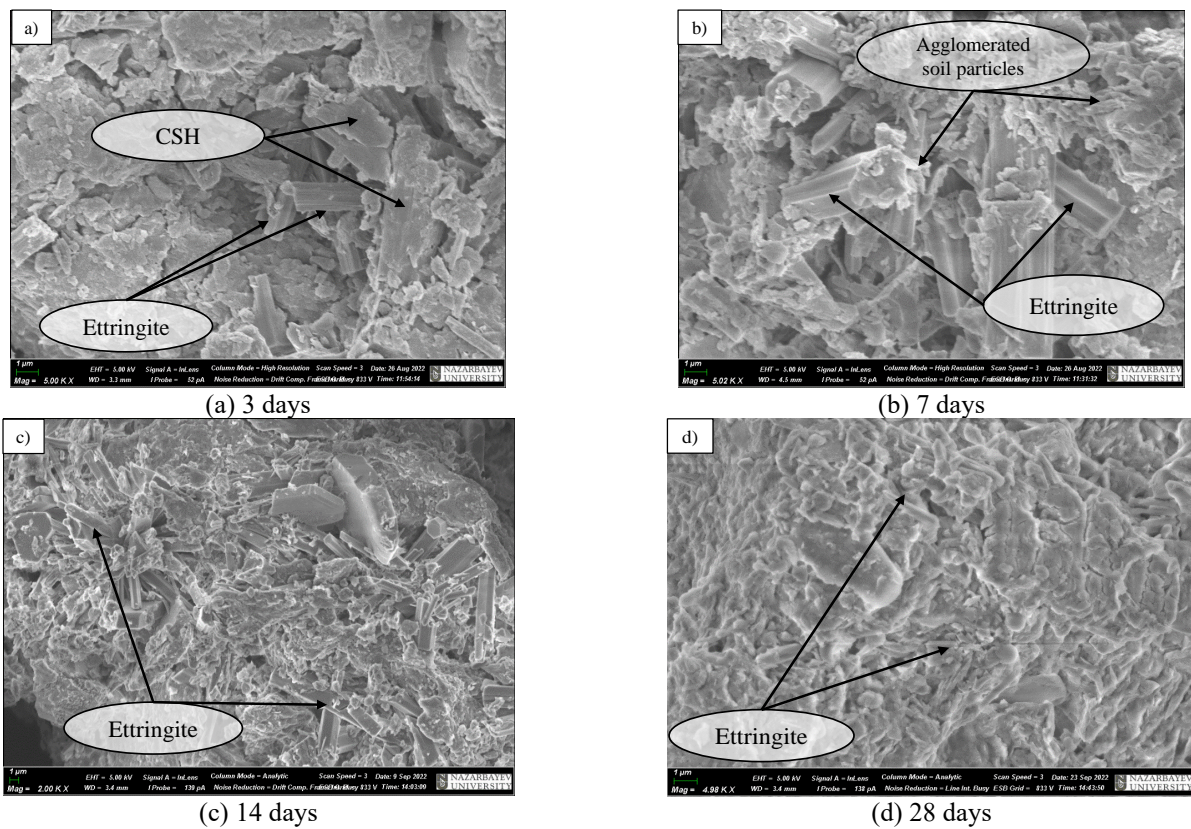


Fig. 13 SEM pictures of 20 % cement treated samples at different curing periods

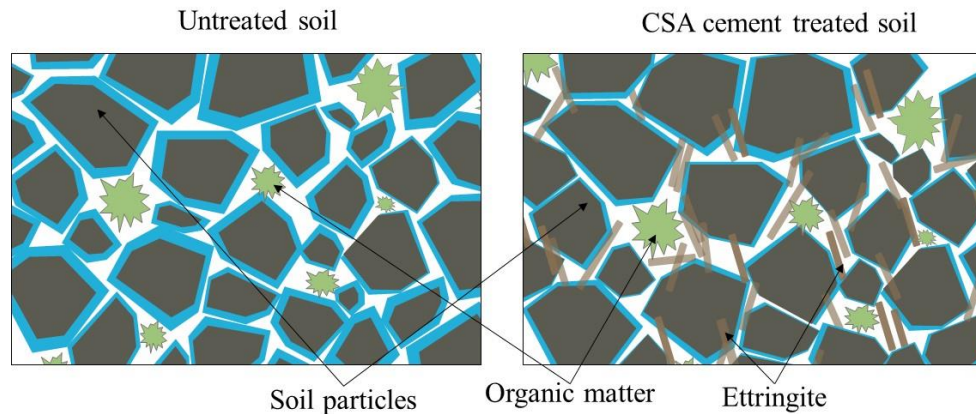


Fig. 14 Formation of needle-like ettringite

- The swelling percentage for the untreated organic soil cured for three days was 7.82%. However, this value decreased with an increased curing period and cement dosage. So, the swelling percentage became negligible, reducing to 0.17% for the 28-day cured sample with 20% cement content.
- The strength gain reaction of treated soil was explained through the hydration process of cement, where ettringite needles filled the spaces, increasing the density and reducing porosity that resulted in early strength gain. It was observed from the SEM pictures, where the changes in the microstructure were shown. Also, these changes were proven with the analysis of FTIR spectroscopy. The absorption peak detected at 1680 cm^{-1} indicates the existence of hydrated products. An increase in the quantity of ettringite, accompanied by a widening of the absorption region due to the presence of O-H groups, can be noted.

Overall, CSA cement is recommended for organic subgrade soil stabilization in terms of rapid strength gain, durability, and environmental friendliness. Moreover, it is crucial to address the potential limitations of this research and explore opportunities to enhance the effectiveness and stability of CSA cement in soil stabilization. This study did not investigate the performance of CSA cement under wet-curing conditions and its long-term impact. Therefore, future research should focus on these areas to improve our understanding and pave the way for the wider use of CSA cement in sustainable soil stabilization practices.

It is critical to recognize the need for a comprehensive study of the long-term effects and impacts of wet curing on organic soil treated with CSA cement. Considering the long-term performance of CSA treated soil allows us to understand its performance over time. In addition, extended exposure to wet curing can optimize the hydration process of cementitious materials within the soil, fostering enhanced strength development over time. Conversely, inadequate or improper wet curing practices may lead to diminished strength gain or uneven strength distribution within the soil mass. Thus, understanding the soil's behavior under wet curing conditions is important for ensuring optimal performance and durability in engineering applications.

Therefore, prioritizing further research into the long-term effects and optimal methodologies of wet curing for organic soils treated with CSA cement is of utmost significance.

Acknowledgments

Funding: This research was funded by the Nazarbayev University, Collaborative Research Project (CRP) Grant No. 11022021CRP1508 and Faculty Development Competitive Research Grant Program (FDCRGP) Grant No. 20122022FD4115. Any opinions, findings, conclusions, or recommendations expressed in this material are those of the author(s) and do not necessarily reflect the views of Nazarbayev University.

References

- Ahmadullah, T. and Chrysochoou, M. (2024), "Relationship between strength development and pozzolanic reactions in lime stabilized kaolinite", *Int. J. Geo-Eng.*, **15**, (1), 11.
- Ale, T.O. (2023), "Improving the geotechnical properties of a Nigerian termite reworked soil using pretest drying conditions and sawdust ash", *Int. J. Geo-Eng.*, **14** (1), 1.
- Arasan, S. and Nasirpur, O (2015), "The effects of polymers and fly ash on unconfined compressive strength and freeze-thaw behavior of loose saturated sand", *Geomech. Eng.*, **8**(3), 361-375. <https://doi.org/10.12989/gae.2015.8.3.361>.
- ASTM/D698 (2021), *Standard Test Methods for Laboratory Compaction Characteristics of Soil Using Standard Effort* American Society for Testing and Materials Internationals; Philadelphia, USA.
- ASTM/D2166 (2006), *Standard test method for unconfined compressive strength of cohesive soil*, American Society for Testing and Materials International; Philadelphia, USA.
- ASTM/D2487 (2000), *Standard Practice for Classification of Soils for Engineering Purposes (Unified Soil Classification System)*, American Society for Testing and Materials Internationals; Philadelphia, USA.
- ASTM/D4546 (2014), *Standard test methods for one-dimensional swell or collapse of soils*, American Society for Testing and Materials Internationals; Philadelphia, USA.
- ASTM/D4829 (2003), *Standard test method for expansion index of soils*, American Society for Testing and Materials

- International; Philadelphia, USA.
- ASTM/D7348 (2013), *Standard test methods for loss on ignition (LOI) of solid combustion residues*, American Society for Testing and Materials International; Philadelphia, USA.
- ASTM/D8295 (2019), *Standard Test Method for Determination of Shear Wave Velocity and Initial Shear Modulus in Soil Specimens Using Bender Elements*, West Conshohocken, PA.
- Bisserik, A., Kim, J., Satyanaga, A. and Moon, S.W. (2021), "Characterization of CSA cemented-treated sands via discrete element method", *Proceedings of the AIP Conference*, Kuala Lumpur, Malaysia, April.
- Bushlaibi, A.H. and Alshamsi, A.M. (2002), "Efficiency of curing on partially exposed high-strength concrete in hot climate", *Cement Concrete Res.*, **32**(6), 949-953. [https://doi.org/10.1016/S0008-8846\(02\)00735-4](https://doi.org/10.1016/S0008-8846(02)00735-4).
- Chen, H. and Wang, Q. (2006), "The behaviour of organic matter in the process of soft soil stabilization using cement", *Bull. Eng. Geol. Environ.*, **65**, 445-448. <https://doi.org/10.1007/s10064-005-0030-1>.
- Chub-uppakarn, T., Chompoorat, T., Thepumong, T., Sae-Long, W., Khamplo, A. and Chairapat, S. (2023), "Influence of partial substitution of metakaolin by palm oil fuel ash and alumina waste ash on compressive strength and microstructure in metakaolin-based geopolymer mortar", *Case Studies in Constr. Mater.*, **19**, e02519. <http://dx.doi.org/10.1016/j.cscm.2023.e02519>.
- Consoli, N.C., Foppa, D., Festugato, L. and Heineck, K.S. (2007), "Key parameters for strength control of artificially cemented soils", *J. Geotech. Geoenviron. Eng.*, **133**(2), 197-205. [https://doi.org/10.1061/\(ASCE\)1090-0241\(2007\)133:2\(197\)](https://doi.org/10.1061/(ASCE)1090-0241(2007)133:2(197)).
- Damtoft, J.S., Lukasik, J., Herfort, D., Sorrentino, D. and Gartner E.M. (2008), "Sustainable development and climate change initiatives", *Cement Concrete Res.*, **38**(2), 115-127. <https://doi.org/10.1016/j.cemconres.2007.09.008>.
- Edil, T.B. and Wang, X. (2000), "Shear strength and K^0 of peats and organic soils", *Geotechnics of high water content materials*, ASTM International.
- Firoozi, A.A., Guney Olgun, C., Firoozi, A.A. and Baghini, M.S. (2017), "Fundamentals of soil stabilization", *Int. J. Geo-Eng.*, **8**, 1-16. <https://doi.org/10.1186/s40703-017-0064-9>.
- García-Gaines, R.A. and Frankenstein, S. (2015), "USCS and the USDA soil classification system: Development of a mapping scheme", ERDC/CRREL; TR-15-4; Engineer Research and Development Center (U.S.)
- Ghadr, S., Assadi Langroudi, A. and Bahadori, H. (2023), "Replacing C_3S cement with PP fibre and nanobiosilica in stabilisation of organic clays", *Geomech. Eng.*, **34**(4), 401-414. <https://doi.org/10.12989/gae.2023.33.4.401>.
- Ghazavi, M. and Roustaei, M. (2010), "The influence of freeze-thaw cycles on the unconfined compressive strength of fiber-reinforced clay", *Cold Reg. Sci. Technol.*, **61**(2-3), 125-131. <https://doi.org/10.1016/j.coldregions.2009.12.005>.
- Gidebo, F.A., Yasuhara, H. and Kinoshita, N. (2023), "Stabilization of expansive soil with agricultural waste additives: a review", *Int. J. Geo-Eng.*, **14**(1), 14.
- Gross, J. and Adaska, W. (2020), "Guide to cement-stabilized subgrade soils", Portland Cement Association: Washington, DC, USA.
- Güllü, H. and Fedakar, H.I. (2017), "Unconfined compressive strength and freeze-thaw resistance of sand modified with sludge ash and polypropylene fiber", *Geomech. Eng.*, **13**(1), 25-41. <https://doi.org/10.12989/gae.2017.13.1.025>.
- Hanein, T., Galvez-Martos, J.L. and Bannerman, M.N. (2018), "Carbon footprint of calcium sulfoaluminate clinker production", *J. Cleaner Product.*, **172**, 2278-2287. <https://doi.org/10.1016/j.jclepro.2017.11.183>.
- Horpibulsuk, S., Katkan, W., Sirilerdwattana, W. and Rachan, R. (2006), "Strength development in cement stabilized low plasticity and coarse grained soils: Laboratory and field study", *Soils Found.*, **46**(3), 351-366. <https://doi.org/10.3208/sandf.46.351>.
- Horpibulsuk, S., Rachan, R., Chinkulkijniwat, A., Raksachon, Y. and Suddepong, A. (2010), "Analysis of strength development in cement-stabilized silty clay from microstructural considerations", *Constr. Build. Mater.*, **24**(10), 2011-2021. <https://doi.org/10.1016/j.conbuildmat.2010.03.011>
- Huang, P.T., Patel, M., Santagata, M.C. and Bobet, A. (2009), "Classification of organic soils", *Publication FHWA/IN/JTRP-2008/02*. <https://doi.org/10.5703/1288284314328>.
- Ifediniro, C. and Ekeocha, N.E. (2022), "Performance of cement-stabilized weak subgrade for highway embankment construction in Southeast Nigeria", *Int. J. Geo-Eng.*, **13**(1), 1. <https://doi.org/10.1186/s40703-021-00166-z>.
- Jexembayeva A, Salem T, Jiao P, Hou B, Niyazbekova R (2020), "Blended cement mixed with basic oxygen steelmaking slag (BOF) as an alternative green building material", *Materials*, **13**, (14), 3062. <https://doi.org/10.3390/ma13143062>
- Jumassultan, A., Sagidullina, N., Kim, J., Ku, T. and Moon, S.W. (2021), "Performance of cement-stabilized sand subjected to freeze-thaw cycles", *Geomech. Eng.*, **25**(1), 41-48. <https://doi.org/10.12989/gae.2021.25.1.041>.
- Kamruzzaman, A., Chew, S. and Lee, F. (2009), "Structuration and destructuration behavior of cement-treated Singapore marine clay", *J. Geotech. Geoenviron. Eng.*, **135**(4), 573-589. [https://doi.org/10.1061/\(ASCE\)1090-0241\(2009\)135:4\(573\)](https://doi.org/10.1061/(ASCE)1090-0241(2009)135:4(573)).
- Khan, Q., Moon, S.W. and Ku, T. (2020), "Idealized sine wave approach to determine arrival times of shear wave signals using bender elements", *Geotech. Test. J.*, **43**(1), 171-193. <https://doi.org/10.1520/GTJ20170121>.
- Ku, T., Subramanian, S. and Moon, S. (2020), "Effect of Gypsum on the strength of CSA treated sand", *Proceedings of the 16th Asian Regional Conference on Soil Mechanics and Geotechnical Engineering, ARC 2019*, Taipei, Taiwan, October.
- Ladd, R. (1978), "Preparing test specimens using undercompaction", *Geotech. Test J.*, **1**(1), 16-23. <https://doi.org/10.1520/GTJ10364J>.
- Ma, C. and Zhang, F.H. (2014), "Analysis and improvement on output current quality of active clamped flyback type micro PV inverters", *Proceedings of the CSEE*, US, July.
- Mekonnen, E., Amdie, Y., Etefa, H., Tefera, N. and Tafesse, M. (2022), "Stabilization of expansive black cotton soil using bioenzymes produced by ureolytic bacteria", *Int. J. Geo-Eng.*, **13**(1), 10.
- Mitchell, J.K. and Soga, K. (2005), "Fundamentals of soil behavior", John Wiley & Sons New York.
- Moon, S.W., Vioth, G., Subramanian, S., Kim, J. and Ku, T. (2020), "Effect of fine particles on strength and stiffness of cement treated sand", *Granular Matter.*, **22**(1), 9. <https://doi.org/10.1007/s10035-019-0975-6>.
- Mustafayeva, A., Bimyikova, A., Olagunju, S.O., Kim, J., Satyanaga, A. and Moon, S.W. (2023), "Mechanical properties and microscopic mechanism of Basic Oxygen Furnace (BOF) slag-treated clay subgrades", *Buildings*, **13**(12), 2962. <https://doi.org/10.3390/buildings13122962>.
- Myślińska, E. (2003), "Classification of organic soils for engineering geology", *Geol. Quart.*, **47**, 39-42.
- Niazi, Y. and Jalili, M. (2009), "Effect of Portland cement and lime additives on properties of cold in-place recycled mixtures with asphalt emulsion", *Constr. Build. Mater.*, **23**(3), 1338-1343. <https://doi.org/10.1016/j.conbuildmat.2008.07.020>.
- Ocheme, J.I., Olagunju, S.O., Khamitov, R., Satyanaga, A., Kim, J. and Moon, S.W. (2023), "Triaxial shear behavior of calcium sulfoaluminate (CSA)-treated sand under high confining pressures", *Geomech. Eng.*, **33**(1), 41-51.

- <https://doi.org/10.12989/gae.2023.33.1.041>.
- Olagunju, S.O., Mukhtarkhan, D., Kim, J., Satyanaga, A. and Moon, S.W. (2023), “Physical, mechanical, chemical, and environmental characterization of stockpiled BOF slag as railway ballast material”, *Constr. Build. Mater.*, **408**, 133613. <https://doi.org/10.1016/j.conbuildmat.2023.133613>.
- Phanikumar, B. (2009), “Effect of lime and fly ash on swell, consolidation and shear strength characteristics of expansive clays: a comparative study”, *Geomech. Geoeng.*, **4**(2), 175-181. <https://doi.org/10.1080/17486020902856983>.
- Pooni, J., Robert, D., Giustozzi, F., Setunge, S., Xie, Y. and Xia, J. (2020), “Novel use of calcium sulfoaluminate (CSA) cement for treating problematic soils”, *Constr. Build. Mater.*, **260**, 120433. <https://doi.org/10.1016/j.conbuildmat.2020.120433>.
- Prusinski, J.R. and Bhattacharja, S. (1999), “Effectiveness of Portland cement and lime in stabilizing clay soils”, *Transport. Res. Record*, **1652**(1), 215-227. <https://doi.org/10.3141/1652-28>.
- Puppala, A.J., Intharasombat, N. and Vempati, R.K. (2005), “Experimental studies on ettringite-induced heaving in soils”. *J. Geotech. Geoenviron. Eng.*, **131**(3), 325-337. [https://doi.org/10.1061/\(ASCE\)1090-0241\(2005\)131:3\(325\)](https://doi.org/10.1061/(ASCE)1090-0241(2005)131:3(325)).
- Regasa, H., Jothimani, M. and Oyda, Y. (2023), “Subgrade soil stabilization using the Quicklime: a case study from Modjo-Hawassa highway, Central Ethiopia”, *Int. J. Geo-Eng.*, **14**(1), 17.
- Sagidullina, N., Abdialim, S., Kim, J., Satyanaga, A. and Moon, S.W. (2022), “Influence of freeze–thaw cycles on physical and mechanical properties of cement-treated silty sand”, *Sustainability*, **14**(12), 7000. <https://doi.org/10.3390/su14127000>.
- Saride, S., Puppala, A.J. and Chikyala, S.R. (2013), “Swell-shrink and strength behaviors of lime and cement stabilized expansive organic clays”, *Appl. Clay Sci.*, **85**, 39-45.
- Sridharan, A. and Prakash, K. (2000), “Shrinkage limit of soil mixtures”, *Geotech. Test J.*, **23**(1), 3-8. <https://doi.org/10.1520/GTJ11118J>.
- Subramanian, S., Moon, S.W., Moon, J. and Ku, T. (2018), “CSA-treated sand for geotechnical application: microstructure analysis and rapid strength development”, *J. Mater. Civil Eng.*, **30**(12), 04018313. [https://doi.org/10.1061/\(ASCE\)MT.1943-5533.0002523](https://doi.org/10.1061/(ASCE)MT.1943-5533.0002523).
- Tremblay, H., Duchesne, J., Locat, J. and Leroueil, S. (2002), “Influence of the nature of organic compounds on fine soil stabilization with cement”, *Can. Geotech. J.*, **39**(3), 535-546. <https://doi.org/10.1139/t02-002>.
- Vinoth, G., Moon, S.W., Kim, J. and Ku, T. (2018), “Effect of fine particles on cement treated sand”. *Proceedings of China-Europe Conference on Geotechnical Engineering*.
- Vinoth, G., Moon, S.W., Moon, J. and Ku, T. (2018), “Early strength development in cement-treated sand using low-carbon rapid-hardening cements”, *Soils Found.*, **58**(5), 1200-1211. <https://doi.org/10.1016/j.sandf.2018.07.001>.
- Wei, X., Liu, H., Choo, H. and Ku, T. (2022), “Correlating failure strength with wave velocities for cemented sands from the particle-level analysis”, *Soil Dyn. Earthq. Eng.*, **152**, 107062. <https://doi.org/10.1016/j.soildyn.2021.107062>.
- Winnefeld, F. and Lothenbach, B. (2010), “Hydration of calcium sulfoaluminate cements—Experimental findings and thermodynamic modelling”, *Cement Concrete Res.*, **40**(8), 1239-1247. <https://doi.org/10.1016/j.cemconres.2009.08.014>.
- Zhang, Y., Johnson, A.E. and White, D.J. (2016), “Laboratory freeze–thaw assessment of cement, fly ash, and fiber stabilized pavement foundation materials”, *Cold Reg. Sci. Technol.*, **122**, 50-57. <https://doi.org/10.1016/j.coldregions.2015.11.005>.
- Zivari, A., Siavoshnia, M. and Rezaei, H. (2023), “Effect of lime-rice husk ash on geotechnical properties of loess soil in Golestan province, Iran”, *Int. J. Geo-Eng.*, **14**, (1), 20.

IC